Statistical analysis of ionic current fluctuations in membrane channels

Szymon Mercik* and Karina Weron†
Institute of Physics, Wroclaw University of Technology, 50-370 Wroclaw, Poland

Zuzanna Siwy‡
Department of Physical Chemistry and Technology of Polymers, Silesian University of Technology, 44-100 Gliwice, Poland

(Received 9 July 1999)

The statistical analysis of an ionic current signal recorded from a single channel of a biological membrane is presented. We find the main characteristics of the ionic current probability density, the closed- and open-state distributions, and the autocorrelation function of the current recordings by using procedures based on the kernel and tail estimators, the bootstrap methodology; and the Zipf plots. The results provide evidence for the non-Markovian character of the channel kinetics of the investigated data. [S1063-651X(99)12812-5]

PACS number(s): 87.17.−d, 05.40.−a

I. INTRODUCTION

Ion channels, i.e., large proteins that are located in the membranes of both plant and animal cells, facilitate the transport of selected ions in and out of the cells. The channels are not permanently open for the conduction of ions but continuously switch between closed and open states. The internal state of the channel undergoes continuous changes, which result from the constantly varying environment: random thermal fluctuations, variations of the voltage difference across the cell membrane, conformational changes of channel proteins, etc.

The ion currents belong to the group of the most vitally important biophysical processes in living cells [1–3]. The determination of their nature is necessary for an understanding of the membrane channel kinetics. Usually, the single channel recordings are analyzed in terms of models assuming that the channel kinetics is a Markov process over a small number of discrete states [4–12]. The assumption that the basic kinetics is purely random can be, however, questioned [13]. The suggestion of the non-Markovian character of channel currents can be found also in [9]. On the other hand, there are evidently the cases where the Markovian nature of the potassium current through single channels was detected [14]. The problem of the detailed statistical characteristics of ion currents is of importance for many reasons [15–26] and has to be solved in order to find realistic models of channels action.

The idea of testing the Markov vs non-Markov condition in ion channel recordings was put forward recently by Timmer and Klein [13]. The statistical test proposed by them, demonstrated on simulated data, is, however, rather indirect and not simple to use. A new method of testing Markovianity was proposed by Fulinski *et al.* [1]. They used a definition of the Markov process based on the Smoluchowski-Chapman-Kolmogorov equation. The method, being very clear and convenient to apply, does not, however, give information on the detailed characteristics of the non-Markovian process.

In this paper we study the statistical properties of real data sets (the same as in [1]). We give ''prescriptions'' for analyzing any long enough time series (in this case, current vs time) by means of which not only the non-Markovian (or Markovian) character of the investigated current signal is brought to light, but also the statistical characteristics related to it can be seen.

II. STATISTICAL INVESTIGATIONS OF THE EXPERIMENTAL DATA

We study a data set that was recorded from cell attached patches of adult locust (*Schistocerca gregaria*) extensor tibiae muscle fibers [1,2]. The muscle preparation was bathed in 180 mM NaCl, 10 mM KCl, 2 mM $CaCl_2$, 10 mM 4-(2-hydroxyethyl)-1-piperazineethanesulphonic acid (HEPES), *p*H 6.8, and the patch pipettes contained 10 mM NaCl, 180 mM KCl, 2 mM $CaCl_2$, 10 mM HEPES, *p*H 6.8. Channel current was recorded using a List EPC-7 Patch-Clamp amplifier. Output was low-pass filtered at 10 kHz, digitized at 22 kHz using Sony PCM ES-701 and stored on standard videotape. Records were transferred to the hard disk of an IBM compatibile PC via an analog-to-digital converter (Axon Instruments) sampling at 10 kHz. The complete data analyzed here should consist of one record composed of $N = 250\,000$ values of the channel current measured at equal intervals $\Delta t = 0.1$ ms, the whole duration being 25 s. The error of measurements of ionic current is equal to $\Delta I = 1$ pA. A sample of the data set is shown in Fig. 1.

A. Probability density of the ionic current signal

To display the frequency with which states along a trajectory of the investigated time series fall into given intervals of current we construct a histogram.

Let us denote the statistical sample by $\{I_i\}_{i=1}^{N}$, where N is the length of the sample. We consider a finite interval $[a,b]$ such that

$$a \leqslant \min_i \{I_i\}$$

*Electronic address: mercik@rainbow.if.pwr.wroc.pl
†Electronic address: karina@rainbow.if.pwr.wroc.pl
‡Electronic address: siwy@zeus.polsl.gliwice.pl

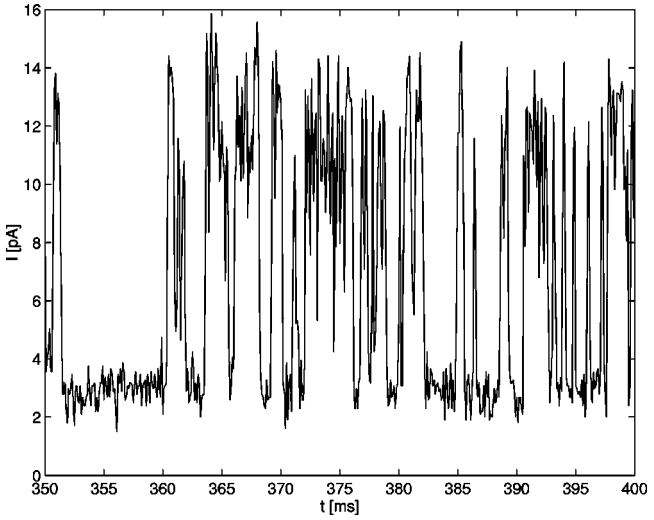

FIG. 1. The original signal of ionic current recorded from a single membrane channel. The data obtained by the courtesy of Professor P. N. R. Ushrewood and Dr. I. Mellor from the University of Nottingham, Nottingham, U.K.

and

$$b \geqslant \max_i \{I_i\}.$$

Next, we divide the interval $[a,b]$ into n nonintersecting subintervals of equal length $h=(b-a)/n$. A histogram is a function $f_{N,n}=f_{N,n}(x)$, constant on each of the subintervals $[x_k,x_{k+1})$, $k=1,2,\ldots n$, and defined as follows:

$$f_{N,n}(x)=\frac{\mathbf{N}\{I_i\in[x_k,x_{k+1}):x\in[x_k,x_{k+1})\}}{nh},$$

where $\mathbf{N}\{\cdots\}$ counts the number of data values falling into the specified intervals of the current.

The histogram (see Fig. 2) gives a rough aproximation of the unknown probability density $f(x)$ of the ionic current signal. The best convergence to the searched density function

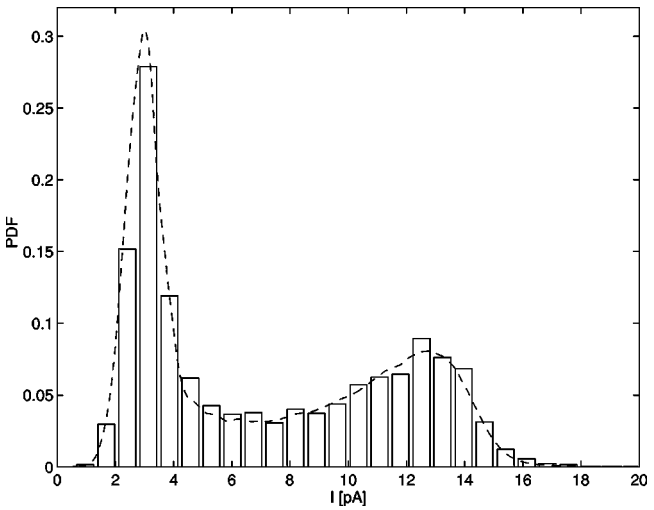

FIG. 2. The histogram (solid line) and the kernel estimator (dashed line) of ionic current probability density.

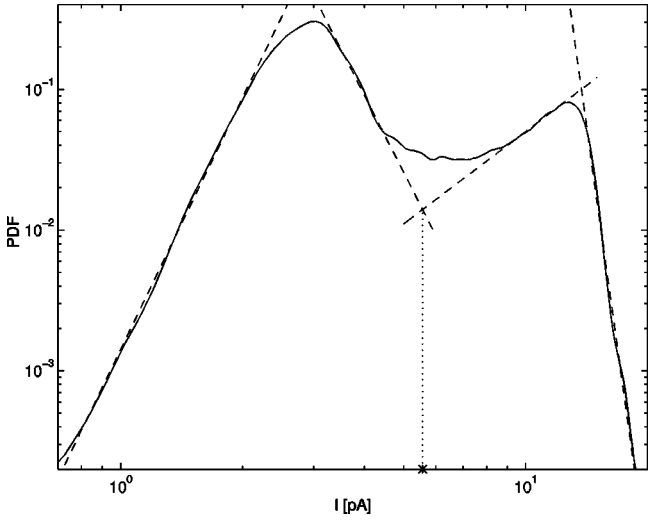

FIG. 3. The ionic current empirical probability density in the log-log scale. The dashed lines represent power laws fulfilled by the branches of low- and high-intensity current peaks. The threshold current is marked by the star.

is obtained if the number of subintervals, n, is proportional to the cube root of the number of observations, N: $n\propto\sqrt[3]{N}$.

A better approximation of the probability density function $f(x)$ may be obtained by means of the kernel density estimator technique introduced by Rosenblatt and Parzen [27,28]. For any real x the kernel density estimator provides an approximate value of the density in the form

$$\hat{f}_N(x)=\frac{1}{N}\sum_{i=1}^{N}\frac{1}{b_N}K\left(\frac{x-I_i}{b_N}\right).$$

The kernel $K(u)$ is a continuous, non-negative, and symmetric function satisfying

$$\int_{-\infty}^{\infty}K(u)du=1,$$

whereas the window $\{b_N\}_{N=1,2,3,\ldots}$ is a sequence of positive real numbers such that $\lim_{N\to\infty}b_N=0$ and $\lim_{N\to\infty}Nb_N=\infty$. In our estimation procedures we used the Bertlett kernel

$$K(u)=\begin{cases}\frac{3}{4}(1-u^2) & \text{if } u\in[-1,1],\\ 0 & \text{if } u\notin[-1,1],\end{cases}$$

with $b_N=10.25\sigma N^{-0.34}$, where σ is the standard deviation of the sample, as it seemed to give the best results. The obtained density is shown in Fig. 2. Note that the kernel density estimator is a smooth and continous function while the histogram is very rough and sensitive to a number of considered intervals.

It is obvious from Fig. 2 that there are two modes of the current. In order to find the properties of this dichotomous distribution we plot the kernel estimator of the probability density in a log-log scale (Zipf plot [29]). The result is presented in Fig. 3. The log-log plot reveals the general features of the current probability density. It is seen that the distinctly bimodal function can be regarded as a superposition of two unimodal densities with clearly pronouced power laws. The

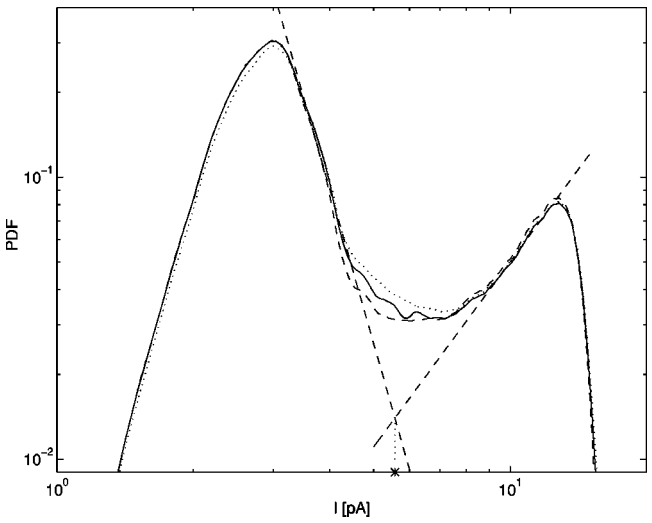

FIG. 4. The ionic current empirical probability density in the log-log scale (solid line) and two densities obtained for different parts of the original signal. The dashed lines represent power laws fulfilled by the branches of low- and high-intensity current peaks. The threshold current is marked by the star.

original experimental series can be hence split into two distinct groups of states, the left one (lower values of the current) interpreted as the closed state and the right one as the open state. The data set was checked by dividing the whole record into smaller subrecords. It has been found that the power laws of the component distributions are almost constant and do not depend on the number of observations taken into account, while the shape of the ionic density estimator changes [particulary the position of the minimum between the peaks moves quite unpredictably (Fig. 4)].

The statistical propetries of the sample record (Fig. 1) can be easily derived if we ''translate'' the record into a dichotomous 0-1 signal. The dichotomous signal can be obtained by separating the current values into two groups of states with respect to the threshold current I^*: the closed one for $I<I^*$ and the open one for $I>I^*$. We put 0 for the closed states and 1 otherwise. The threshold I^* cannot be, however, equal to the value of the current for which the density estimator takes minimum. The position of the minimal value of the estimator varies with the sample and the sample's size (see Fig. 4). Our methodology of finding I^* is based on the weak dependence of the power laws of the component densities on the sample taken from the original experimental series. We assume the threshold I^* to be equal to the current's value for which the power laws intersect (see Fig. 3). The result is shown in Fig. 5, where the threshold $I^*=5.6\pm0.2$ pA. Note that the difference in the I^* values obtained here and in [1] (i.e., 5.0 ± 0.2 pA) results from using different methods of the threshold determination. That also influenced statistic properties of the dichotomous signal; e.g., the number of distinguished closed and open states has been increased by 4%.

The mean value of the current in the closed states is equal to

$$\langle I_c\rangle = 3.2\pm0.1 \text{ pA}$$

and in the open states

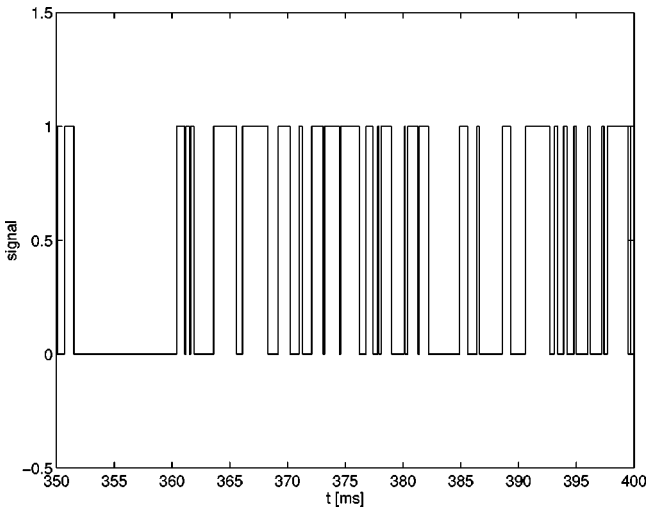

FIG. 5. The 0-1 signal representing closed (0) and open (1) states of the ionic channel; dichotomous representation of time series presented in Fig. 1.

$$\langle I_o\rangle = 11.0\pm0.1 \text{ pA},$$

where $\langle\ \rangle$ denotes the arithmetic mean. The mean values of the closed-T_c and open times T_o are equal:

$$\langle T_c\rangle = 0.84\pm0.01 \text{ ms}, \tag{2.1}$$

$$\langle T_o\rangle = 0.79\pm0.01 \text{ ms}, \tag{2.2}$$

while the maximum values of the closed and open times, given with the experimental error, are

$$\max\{T_c\} = 300.8\pm0.1 \text{ ms}$$

and

$$\max\{T_o\} = 27.2\pm0.1 \text{ ms},$$

respectively.

B. Tail properties of closed- and open-time distributions

To investigate the closed- and open-time distributions let us introduce the notion of a distribution's tail. The tail of the distribution $F(t)$ of a random variable T with the probability density $f(t)$ is defined as [30]

$$P\{T>t\} = 1-F(t) = \int_t^\infty f(T)dT.$$

The tail properties of the distribution $F(t)$ can be revealed by constructing the tail estimator

$$1-\hat{F}(t) = \frac{\mathbf{N}\{T_i>t\}}{M} \tag{2.3}$$

for a sample $\{T_i\}_{i=1}^M$ of the closed and open times, respectively, and representing it by means of the log-log plot. The result is shown in Fig. 6. The straight lines (for $t\gg1$) clearly indicate the power-law behavior t^{-D} for both the closed- and open-time distributions with the exponent D determinated by the slope of the line

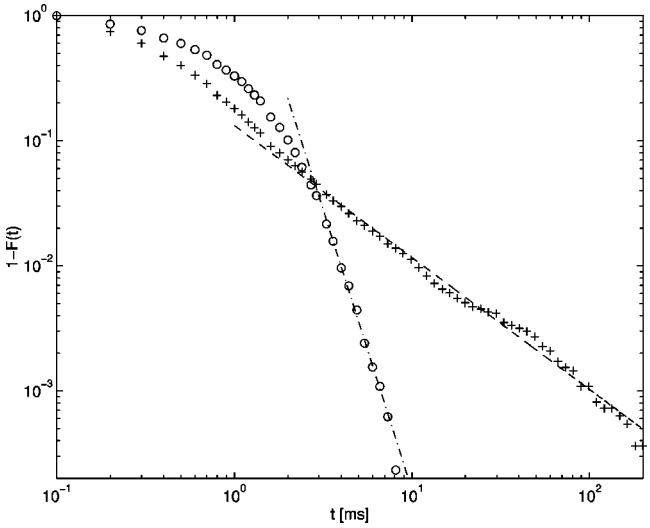

FIG. 6. The tails of the closed- (crosses) and open-time (circles) distributions in log-log scale with fitted lines (dashed line for the closed- and dash-dotted line for the open-time distribution tail).

$$D_c = 1.24 \pm 0.04$$

and

$$D_o = 3.85 \pm 0.19.$$

The heavier tail belongs to the closed-time distribution.

The precise value of the exponent D can be found with help of the Hill estimator. The estimator of the exponent D is given by

$$\hat{D}_{M,m} = \frac{1}{\hat{\gamma}_{M,m}},$$

where

$$\hat{\gamma}_{M,m} = \frac{1}{m} \sum_{i=1}^{m-1} \log T_{(i)} - \log T_{(m)}, \tag{2.4}$$

and $m < M$ is a positive integer which determines the length of the sample taken into account in the calculations. The above procedure applies to the statistical sample $\{T_i\}_{i=1}^{M}$ rearranged in a nondecreasing order, i.e., $T_{(1)} \leqslant T_{(2)} \leqslant T_{(3)} \leqslant \cdots \leqslant T_{(M)}$. To improve the calculations we had to use the Hill estimator for bootstrap samples consisting of 100 000 elements. The bootstap methodology [31] helps us to refine the time discretization. (The shortest time interval in the experimental record is equal to 0.1 ms, that is, about 1/8 of the mean value of closed and open times.) The dependence of the tail estimator on the length m of sample taken into calculation is presented in Fig. 7. One can observe that there is an interval of stabilization of the estimator value after high volatility interval for small m. The power-law exponents derived by means of the Hill estimator are

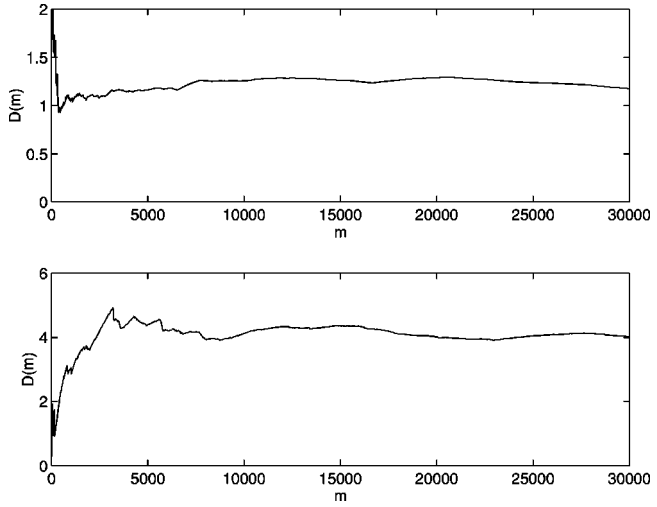

FIG. 7. Dependence of the Hill estimator values of the exponent D for closed- (top) and open-time states (bottom) upon the sample length m.

$$D_c = 1.25 \pm 0.03$$

and

$$D_o = 4.16 \pm 0.17$$

for the closed and open times, respectively. Note that for the larger power exponent related to the open states the volatility is greater. This occurs because the larger power-law exponents are more sensitive to fluctuations of single points in approximations.

C. Short- and long-range correlation properties of the ionic current signal

The autocorrelation function $\kappa(s,t)$ of the ionic current signal $\{I_t\}_{t=1}^{T}$ is defined as

$$\kappa(s,t) = \frac{\langle (I_s - \mu_s)(I_{s+t} - \mu_{s+t}) \rangle}{\sigma_s \sigma_{s+t}},$$

where σ_s is a standard deviation and μ_s is the mean value of the sample at the moment s [30]. If we assume that the series' properties are stationary in time, we get that the autocorrelation function is given by

$$\kappa(t) = \kappa(s,t) = \frac{\langle I_s I_{s+t} \rangle - \mu^2}{\sigma^2};$$

i.e., it is independent of the moment s of the initial observation. Here μ is the mean value of the sample and σ^2 is the sample's variation. The stationarity of the record was checked by dividing it into few smaller subrecords and by calculating the statistical properties for every subrecord sepa-

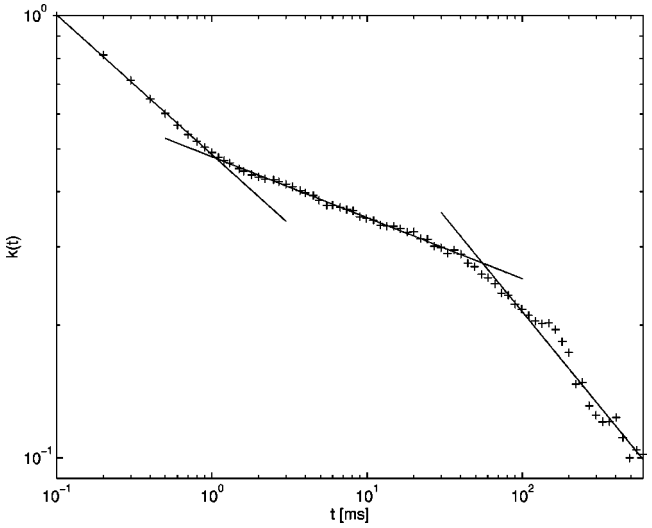

FIG. 8. The autocorrelation function of the ionic current signal.

rately. It was found that the results were similar (within experimental error) for every subrecord and for the whole time series.

The autocorrelation function $\kappa(t)$ is plotted in Fig. 8. One can easily distinguish three intervals of different behavior of the autocorrelation function: the first one for $t<1$ ms, the second one for 1 ms$<t<40$ ms, and the third one for $t>40$ ms. The autocorrelation function decreases with power laws in all intervals, but the power exponent is different in each of them. The power laws are

$$\kappa(t)\propto\begin{cases} t^{-0.32\pm0.04} & \text{for} \quad t<1 \text{ ms}, \\ t^{-0.14\pm0.02} & \text{for} \quad 1 \text{ ms}<t<40 \text{ ms}, \\ t^{-0.55\pm0.10} & \text{for} \quad t>40 \text{ ms}. \end{cases} \tag{2.5}$$

The autocorrelation function can be treated as a measure of memory in the system while its exponents give information on the speed of correlation loss between states separated in time. The first scaling region extends to 1 ms, which is of the same order of magnitude as the average opening and closing times (0.79 and 0.84 ms, respectively). It describes, therefore, the correlation falloff while the system stays in one state: open or closed. For t belonging to (1,40) ms the correlation function scales with exponent 0.14 ± 0.02. A low value of the exponent assures a slow correlation fall. As t here is larger than the sum of average opening and closing times, and also than the longest open time duration, the second scaling region of $\kappa(t)$ function describes the long-range correlation between subsequent, different states of the channel. Note that for t equal to 40 ms the autocorrelation function still takes a high value. The third region of $\kappa(t)$ scaling shows the fastest correlation falloff.

The observed behavior of the autocorrelation function, revealing the existence of long-range correlation (memory) in the system, clearly indicates the non-Markovianity of the time series behavior examined. Bassignhwaite *et al.* point out [14] the possibility of using the autocorrelation function in an estimation of the fractal dimension of a time series. The fractal nature of ion-channel activity has also been described in [32]. For a signal occurring in one dimension, the fractal dimension d lies between 1 and 2. The fractal dimension d and the exponent of autocorrelation scaling, D_κ, are related by a simple, linear formula [14]

$$d=1+\frac{D_\kappa}{2}. \tag{2.6}$$

d belonging to the range 1–1.5 indicates a positive correlation between the nearest-neighbor points. When there is no correlation in the system d is equal to 1.5; d higher than 1.5 indicates a negative correlation between neighboring values.

The fractal dimension, calculated on the basis of Eq. (2.6), for three different scaling regions of the autocorrelation function is equal to

$$d=\begin{cases} 1.16\pm0.02 & \text{for} \quad t<1 \text{ ms}, \\ 1.07\pm0.01 & \text{for} \quad 1 \text{ ms}<t<40 \text{ ms}, \\ 1.27\pm0.05 & \text{for} \quad t>40 \text{ ms}. \end{cases} \tag{2.7}$$

The fractal dimension suggests, therefore, the existence of a positive correlation in the system.

III. CONCLUSIONS

The main objective of the paper was to get information on the nature and statistical characteristics of potassium current through a locust potassium channel [1,2]. In the analysis we have applied widely used statistical tools, which we, however, enriched and modified. The probability density function (PDF) has been found through the application of the kernel density estimator technique rather than the more popular but noncontinuous histogram. The usefulness of the analysis of the PDF in log-log coordinates has been emphasized. It allowed us to discover power-law scaling at the closed and open states distributions. The exponents of PDF scaling appeared to be surprisingly ''stable'' and independent of the number of observations considered. Power laws have also been found in dwell-time distributions (open and closed). Application of the Hill estimator and the bootstrap methodology allowed us to get precise values of the exponents. We have also examined short- and long-time correlation in the system by means of the autocorrelation function. Three regions of the autocorrelation function with different power-law decays have been clearly distinguished. Low values of the exponents up to 40 ms assure slow correlation falloff and the existence of memory in the system. The non-Markovian character of the experimental data of potassium current, examined already in [1], has been, therefore, confirmed. The question, which appears in this context, is which physical phenomena may be responsible for observed ionic current behavior? One has to take into account that recorded current represents a response of the whole system, consisting of ions and the channel, to an external stimuli (voltage in the examined case). The non-Markovian character of the recorded data may result, therefore, from interactions between channel structure and ions inside the channel. An influence of internal adsorption [33], ''a crowding'' of ions inside narrow pores [34,35], and of conformational changes of polymers chains [36] has already been pointed out. The state of the

whole system, being a result of interactions between ions and between ions and the channel, can influence the future history of the system, seen as a high value of the correlation.

We would like to emphasize that the statistical analysis presented in this paper can be applied to any long enough time series, and enable one to get information on the main statistical characteristics and the nature of the physical process examined.

ACKNOWLEDGMENTS

We are grateful to Professor P. N. R. Usherwood and Dr. I. Mellor from the University of Nottingham for providing us with the experimental data of ion current through a high-conductance locust potassium channel. Part of this work (Z.S.) was done under Silesian University of Technology Grant No. BW-430/RCh4/99.

[1] A. Fuliński, Z. Grzywna, I. Mellor, Z. Siwy, and P. N. R. Usherwood, Phys. Rev. E **58**, 919 (1998).
[2] E. Gorczyńska, P. L. Huddie, B. A. Miller, I. R. Mellor, R. L. Ramsey, and P. N. R. Usherwood, Pflügers Arch. Ges. Physiol. Menschen Tiere **432**, 597 (1996).
[3] J. W. Mozrzymas, M. Martina, and F. Ruzzier, Pflügers Arch. **433**, 413 (1997).
[4] E. Neher and B. Sakmann, Nature (London) **260**, 799 (1976).
[5] J. B. Patlak, K. A. F. Gration, and P. N. R. Usherwood, Nature (London) **278**, 643 (1979).
[6] *Single Channel Recordings*, edited by B. Sakmann and E. Neher (Plenum Press, New York, 1983).
[7] L. S. Liebovitch, J. Stat. Phys. **70**, 329 (1993).
[8] L. J. de Felice and A. Isaac, J. Stat. Phys. **70**, 339 (1993).
[9] D. Petracchi, C. Ascoli, M. Barbi, S. Chillemi, M. Pellegrini, and M. Pellegrino, J. Stat. Phys. **70**, 393 (1993).
[10] D. Colquhoun and A. G. Hawkes, Proc. R. Soc. London, Ser. B **211**, 205 (1981).
[11] R. Horn, in *Ion Channels: Molecular and Physiological aspects*, edited by W. D. Stein (Academic Press, New York, 1984).
[12] A. L. Blatz and K. L. Magleby, J. Physiol. (London) **378**, 141 (1986).
[13] J. Timmer and S. Klein, Phys. Rev. E **55**, 3306 (1997).
[14] J. B. Bassingthwaighte, L. S. Liebovitch, and B. J. West, *Fractal Physiology* (Oxford University Press, Oxford, 1994).
[15] B. Robertson and R. D. Astumian, Biophys. J. **57**, 689 (1990).
[16] V. S. Markin, T. Y. Tsong, R. D. Astumian, and B. Robertson, J. Chem. Phys. **93**, 5062 (1990).
[17] V. S. Markin and T. Y. Tsong, Biophys. J. **59**, 1308 (1991).
[18] B. Robertson and R. D. Astumian, J. Chem. Phys. **94**, 7414 (1991).
[19] A. Fuliński, Phys. Rev. Lett. **79**, 4926 (1997); Chaos **8**, 549 (1998).
[20] J. A. Fay, Phys. Rev. E **56**, 3460 (1997).
[21] E. Di Cera and P. E. Phillipson, J. Chem. Phys. **93**, 6006 (1990).
[22] M. Schienbein and H. Gruler, Phys. Rev. E **56**, 7116 (1997).
[23] F. Moss and X. Pei, Nature (London) **376**, 211 (1995).
[24] S. M. Bezrukov and I. Vodyanoy, Nature (London) **378**, 362 (1995); **385**, 319 (1997), Biophys. J. **73**, 2456 (1997).
[25] J. J. Collins, C. C. Chow, and T. T. Imhoff, Nature (London) **376**, 236 (1995); Phys. Rev. E **52**, R3321 (1995).
[26] D. J. Christini and J. J. Collins, Phys. Rev. Lett. **75**, 2782 (1995).
[27] L. Devroye, *A Course on Density Estimation* (Birkhäuser, Boston, 1987).
[28] A. Janicki and A. Weron, *Simulation and Chaotic Behavior of α-Stable Stochastic Processes* (Marcel Dekker, New York, 1994).
[29] G. K. Zipf, *Human Behavior and the Principle of Least Effort* (Addison-Wesley, Reading, MA, 1949).
[30] W. Feller, *An Introduction to Probability Theory and Its Applications*, 2nd ed. (Wiley, New York, 1971).
[31] B. Efron, Ann. Stat. **7**, 1 (1992).
[32] S. B. Lowen, L. S. Liebovitch, and J. A. White, Phys. Rev. E **59**, 5970 (1999).
[33] Z. J. Grzywna, L. S. Liebovitch, and Z. Siwy, J. Membr. Sci. **242**, 235 (1998).
[34] Z. J. Grzywna, Z. Siwy, and C. L. Bashford, J. Membr. Sci. **121**, 261 (1996).
[35] Z. J. Grzywna and Z. Siwy, Int. J. Bifurcation Chaos Appl. Sci. Eng. **5**, 1115 (1997).
[36] M. Karplus and J. A. McCammon, Annu. Rev. Biochem. **53**, 263 (1983).